Isoform B of myosin II heavy chain mediates actomyosin contractility during TNFα-induced apoptosis

Sara Solinet and María Leiza Vitale*

Department of Pathology and Cell Biology, Université de Montréal, 2900 Edouard-Montpetit, Montréal, Québec, H3T 1J4, Canada
*Author for correspondence (e-mail: maria.leiza.vitale@umontreal.ca)

Accepted 19 February 2008
Journal of Cell Science 121, 1681-1692 Published by The Company of Biologists 2008
doi:10.1242/jcs.022640

Summary

Cells that are treated long-term with TNFα or short-term with TGFα together with cycloheximide (CHX) undergo apoptosis. Cell shrinkage and detachment during apoptosis is dependent on actomyosin contractility. Myosin II heavy chain (MHCII) isoforms have shared and distinct functions. Here, we investigated whether the involvement of MHCII isoforms A and B (MHCIIA and MHCIIB, respectively) in cell shrinkage and detachment differs during apoptosis. We show that TNFα induces caspase-dependent MHCIIA degradation, whereas MHCIIB levels and association with the cytoskeleton remained virtually unchanged in TtT/GF cells and NIH 3T3 fibroblasts. MHCIIA proteolysis also occurred in fibroblasts that lack MHCIIB when treated with TNFα and CHX together. The absence of MHCIIB did not affect cell death rate. However, MHCIIB$^{-/-}$ cells showed more resistance to TNFα–induced actin disassembly, cell shrinkage and detachment than wild-type fibroblasts, indicating the participation of MHCIIB in these events. Moreover, inhibition of atypical PKCζ, which targets MHCIIB but not MHCIIA, blocked TNFα-induced shrinkage and detachment in TtT/GF cells and wild-type fibroblasts, but the inhibitory effect was significantly reduced in MHCIIB$^{-/-}$ fibroblasts. TNFα treatment increased cytoskeleton-associated myosin light chain (MLC) phosphorylation but did not induce actin cleavage. In conclusion, our results demonstrate that MHCIIB, together with MLC phosphorylation and actin, constitute the actomyosin cytoskeleton that mediates contractility during apoptosis.

Supplementary material available online at
http://jcs.biologists.org/cgi/content/full/121/10/1681/DC1

Key words: Myosin, Apoptosis, Actin

Introduction

The tumour necrosis factor α (TNFα) is a pro-inflammatory cytokine involved in distinct bioregulatory functions such as cell proliferation, differentiation and programmed cell death or apoptosis (Leong and Kaplan, 2000). During apoptosis, TNFα signalling triggers the trimerisation of TNFα-receptor-1 (TNFR1) leading to the sequential recruitment of a series of adaptor proteins to constitute the death-inducing signalling complex (DISC) (Baud and Karin, 2001). DISC assembly induces the cleavage and activation of the initiator procaspase 8 (Baud and Karin, 2001), which triggers the 'execution phase' of apoptosis during which several effector caspases are activated that cause the cleavage of target proteins (Mills et al., 1999) – amongst them several cytoskeletal proteins (Chen et al., 2001; Jänicke et al., 1998; Kook et al., 2003). The execution phase of the apoptotic process is characterised by specific changes in cell morphology, such as chromatin condensation and fragmentation, cell shrinkage, membrane blebbing, and apoptotic-body formation (Earnshaw, 1995; Mills et al., 1999). Actin-myosin interaction is required to generate the contractile force necessary for most of these morphological responses (Croft et al., 2005; Mills et al., 1999; Suarez-Huerta et al., 2000b).

Myosins are motor proteins that bind to and move on actin filaments. Myosins are oligomers formed by one or two myosin heavy chains (MHCs) and one or more myosin light chains (MLCs). Several classes of myosins have been described and classified on the basis of the MHC isoform in the complex (Korn, 2000). Contractile actomyosin fibers are mainly formed by the association of actin and myosin II. Class II conventional myosins are hexamers constituted through the noncovalent association of a pair of MHCs (MHCII; 200 kDa) and two pairs of MLCs (17 and 20 kDa) one of which is 'regulatory' and the other 'constitutive' (Bresnick, 1999).

Actomyosin fiber contraction in nonmuscle cells is regulated by the phosphorylation state of the regulatory MLC, which is dependent on MLC kinase (MLCK) (Gallagher et al., 1997), the Rho-regulated kinases (ROCK1 and ROCK2) (Amano et al., 1996; Maekawa et al., 1999) and on myosin phosphatase (Kimura et al., 1996; Noda et al., 1995). All these enzymes are necessary for cell contraction, shrinkage, membrane bleb formation and relocalisation of fragmented DNA into apoptotic bodies (Coleman et al., 2001; Croft et al., 2005; Mills et al., 1998; Orlando et al., 2006; Song et al., 2002).

Experimental evidence has demonstrated a role for MLC phosphorylation and for the corresponding kinases in generating contractile forces within cells that undergo apoptosis, but the potential role of MHC has received little attention. Interaction between actin and myosin II and, thus, the formation of actomyosin contractile elements, also depend on the heavy chains that possess the actin-binding site and the actin-activated ATPase activity (Bresnick, 1999). The C-terminal region of the MHC binds to cellular structures and acts as a crosslinker that stabilises the actomyosin complex (Bresnick, 1999). The class II nonmuscle MHC consists of three isoforms, MHCIIA, MHCIIB (Sellers and

Goodson, 1995) and the recently discovered MHCIIC (Golomb et al., 2004). Whereas MHCIIA and MHCIIB share a high degree of homology in the amino-acid sequence (Takahashi et al., 1992), their catalytic activity and intracellular distribution differ (Kawamoto and Adelstein, 1991; Kelley et al., 1996; Lo et al., 2004). This suggests that, although some of the activities of the isoforms overlap (Wylie and Chantler, 2001), intrinsic differences also occur (Kolega, 2003; Lo et al., 2004; Straussman et al., 2001; Swailes et al., 2006; Togo and Steinhardt, 2004; Vicente-Manzanares et al., 2007; Wei and Adelstein, 2000; Wilson et al., 2001; Wylie and Chantler, 2003). In addition, differential phosphorylation of MHCIIs has been shown to be implicated in regulating myosin fiber assembly (Redowicz, 2001). Numerous studies have focussed on the role of MHCII isoforms in cell locomotion and cytokinesis but few have attempted to elucidate the role of the isoforms in apoptosis. MHCIIA has been reported to be a caspase 3 target during apoptosis (Gerner et al., 2000; Kato et al., 2005; Suarez-Huerta et al., 2000a).

Our study addresses the contribution of MHCII isoforms A and B in actin cytoskeleton remodelling during TNFα-induced apoptosis. The study used the folliculostellate (FS) cell line TtT/GF, a stable mouse cell line characterised by morphological and biochemical features of normal FS cells (Allaerts and Vankelecom, 2005; Inoue et al., 1992). TtT/GF cells express the TNFR1 receptor (Kobayashi et al., 1997) and are responsive to TNFα (Fortin et al., 2006; Kobayashi et al., 1997; Meilleur et al., 2007). Here, we report a distinctive participation of MHCIIA and MHCIIB in the execution phase of apoptosis. MHCIIB, together with the phosphorylated MLCs, is required for the formation of a functional contractile cytoskeleton that is needed for shrinkage and detachment of apoptotic cells. In addition, our results show that PKCζ facilitates this process.

Results

Long-term TNFα treatment induces apoptosis of TtT/GF cells

TtT/GF cells cultured in serum-containing medium possessed abundant lamellipodia, pseudopodia and membrane ruffles and, as they settle, progressively acquired a flatten and elongated morphology (Fig. 1A, control, 24 to 96 hours). We have previously shown that the actin cytoskeleton of serum-cultured TtT/GF cells is characterised by its association with the subplasmalemmal region and by the presence of thin cytoplasmic actin cables (Zheng et al., 2005). Treatment of TtT/GF cells with TNFα for increasing periods of time (0-96 hours) induced the cells to acquire a rounded shape and to detach from the culture support (Fig. 1A, TNFα). Detached cells showed abundant membrane blebbing (Fig. 1A, TNFα, inset). These morphological responses of TtT/GF cells to TNFα were similar to those seen in cells undergoing apoptosis (Earnshaw, 1995; Mills et al., 1999). To confirm or infirm whether long-term TNFα treatment alone caused apoptosis of TtT/GF cells, we searched for the presence of distinct apoptotic hallmarks.

First, by using western blot analysis, we detected the cleavage – and, therefore, the activation – of the initiator caspase 8 (Fig. 1B) and the effector caspase 3 (Fig. 1C) following treatment with TNFα. Caspase 8 activation was observed as early as 48 hours after addition of TNF-α (Fig. 1B), whereas caspase 3 activation was observed from 72 hours onwards (Fig. 1C). Caspase 3 cleavage was blocked by the wide-range caspase inhibitor Z-VAD-fmk (Fig. 1D). Interestingly, the caspase 3 fragment corresponding to the active enzyme was recovered in the cytoskeleton-enriched-fraction of TNFα-treated cells (Fig. 1D), suggesting a close interaction between cytoskeletal proteins and activated caspase 3 during TNFα treatment.

Second, three different methods were used to quantify and determine whether TNFα-treated TtT/GF cells undergo apoptosis: (1) detection and counting of cell nuclei containing condensed chromatin using an assay in which healthy cells show low levels of blue fluorescence, apoptotic cells show high levels of blue fluorescence and necrotic cells show a combination of blue and red fluorescence; (2) measurement of cytoplasmic nucleosome release induced by endonuclease activation using a photometric enzyme-immunoassay that detects cytoplasmic histone-associated-DNA fragments (mono and oligonucleosomes) and; (3) counting of detached cells. Our time-course studies showed that there was an increasing trend in the number of TNFα-treated cells displaying these apoptotic markers from 48 hours onwards (Fig. 1E). TNFα-induced TtT/GF cell contraction and detachment (Fig. 1F), and nucleosome release (Fig. 1G) were blocked by the caspase inhibitor Z-VAD-fmk.

Third, in accordance with the orderly dismantling of the apoptotic cells due to the proteolysis of key structural proteins, exposure of TtT/GF cells to TNFα for more than 48 hours caused the downregulation of the focal-adhesion-associated protein α-actinin and the cleavage of the actin-anchoring protein spectrin into two fragments (Fig. 1H). The 150 kDa spectrin fragment corresponds to the calpain-catalysed cleavage of spectrin, whereas the 120 kDa fragment corresponds to the caspase-3-mediated cleavage of the protein (Boivin et al., 1990; Jänicke et al., 1998). The TNFα-induced proteolysis of these actin-binding proteins was coincident with the activation of caspase 8 and caspase 3, and was blocked by Z-VAD-fmk (not shown).

Fourth, changes in the phosphorylation state of MLC during apoptosis are required for cell retraction, membrane blebbing, nuclear disintegration and the formation of apoptotic bodies (Croft et al., 2005; Mills et al., 1998). We found that MLC phosphorylated at serine residue 19 (MLC-Ser19-*P*) was mainly associated with the cytoskeleton-enriched fraction of control and TNFα-treated cells. Long-term exposure of TtT/GF cells to TNFα increased levels of MLC-Ser19-*P*, which were reduced by caspase inhibition (Fig. 2A). Most MLC was recovered in the cytoskeleton fraction of control and TNFα-treated cells (Fig. 2A). The cytoskeleton-associated MLC levels slightly increased after TNFα treatment and this was independent of caspase activation (Fig. 2A). By contrast, the TNFα-induced MLC decreased in the non-cytoskeleton-enriched fraction was partially blocked by Z-VAD-fmk (Fig. 2A). Long-term incubation with TNFα led to ROCK1 translocation to the cytoskeleton and to its cleavage into a 122 kDa fragment that was also recovered in the cytoskeleton fraction (Fig. 2B). ROCK1 cleavage, but not its translocation to the cytoskeleton, was blocked by caspase inhibition (Fig. 2B). ROCK2 was not cleaved by TNFα treatment (data not shown). The ROCK inhibitor Y-27632 blocked TNFα-induced MLC-Ser19-*P* increase (not shown). ROCK inhibition induced broad lamellipodia and thin cytoplasmic extensions in untreated cells, and blocked TNFα-induced cell contraction and detachment (Fig. 2C). Together, the results prove that long-term TNFα treatment induced the apoptosis of TtT/GF cells. Moreover, the findings demonstrate that there is a time-related activation of caspase 3 and cytoskeleton remodelling in TNFα-induced TtT/GF cell apoptosis.

The role of MHCIIA and MHCIIB in the execution phase of apoptosis

The participation of MLC in apoptosis is well established but the differential implication of the MHCII isoforms is unknown. We

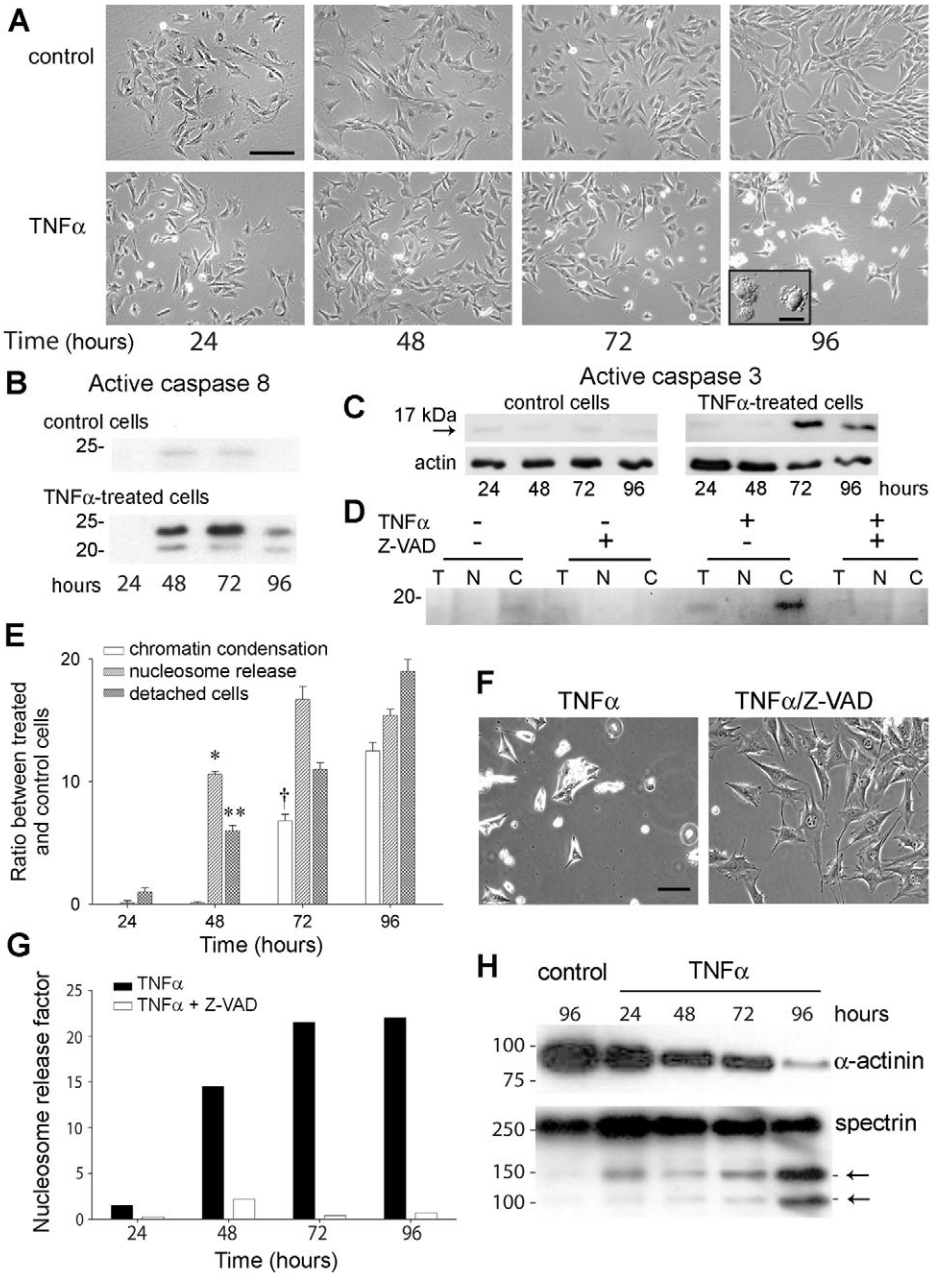

Fig. 1. TtT/GF cell apoptosis following long-term treatment with TNFα. TtT/GF cells were incubated with culture medium alone (control) or with medium containing 20 ng/ml TNFα (TNFα) for increasing periods of time. (A) The phase-contrast micrographs show control TtT/GF cells with a typical morphology of spreading cells with abundant filopodia and lamellipodia. After 48-96 hours in culture, the cells became elongated and lamellipodia became less abundant. Following TNFα treatment, the cells progressively lost the membrane extensions, they shrunk and detached. Scale bar: 250 μm. Inset: Differential interference contrast microscopy shows membrane blebbings of detached cells that had been treated with TNFα for 96 hours. Scale bar: 25 μm. (B) Representative western blots demonstrating the absence and the presence of active caspase 8 in total-cell lysates from control and TNFα-treated cells, respectively. (C) Following treatments, total-cell lysates were obtained and subjected to electrophoresis and western blotting with an antibody that exclusively recognises the active caspase 3 fragment and with anti-actin (loading control). The representative western blots show a 17 kDa band corresponding to the active caspase 3 in cells that had been treated with TNFα for 72 hours and 96 hours, but not in control TtT/GF cells. (D) TtT/GF cells were incubated with either control culture medium or culture medium containing TNFα (20 ng/ml final concentration) both in the absence or in the presence of the caspase inhibitor Z-VADfmk (5 μM, final concentration) for 96 hours. Following treatments, total cell lysates (T), non-cytoskeleton (N) and cytoskeleton (C) fractions were obtained and subjected to electrophoresis and western blotting with an anti-active caspase 3. Cleaved caspase 3 was recovered in the cytoskeleton fraction and the cleavage was blocked by Z-VAD-fmk. (E) Time-course studies showing the increased chromatin condensation (†P<0.001, 72 hours vs 48 hours), nucleosome release (*P<0.0001, 48 hours vs 24 hours) and cell detachment (**P<0.0002, 48 hours vs 24 hours) in TNFα-treated TtT/GF cells. Chromatin condensation in apoptotic cells was evaluated by labelling the cells with Hoechst 33342 and propidium iodide. Nucleosome release was measured by quantifying cytoplasmic histone-associated-DNA fragments (mono and oligonucleosomes). Cell detachment was quantified by counting detached cells with a hemocytometer. Data from three independent experiments are expressed as the ratio of treated to control cells ± s.e.m. (F) TNFα-induced cell shrinkage and detachment were blocked by caspase inhibition (scale bar: 50 μm). (G) TNFα-induced nucleosome release was blocked by the caspase inhibitor Z-VAD-fmk. (H) After incubation with medium alone (control) or containing TNFα for increasing periods of time, total cell lysates were subjected to electrophoresis and western blotting with α-actinin and spectrin antibodies. The representative western blot shows α-actinin downregulation and spectrin cleavage into two fragments of 120 kDa and 150 kDa of molecular mass, respectively (arrows) in TNFα-treated cells.

therefore investigated the participation of MHCIIA and MHCIIB in TNFα-induced TtT/GF cell apoptosis. TtT/GF cells were incubated 96 hours with either with culture medium only or with culture medium containing TNFα. Next, MHCIIA and MHCIIB expression was analysed by western blotting in the non-cytoskeleton (N)- and cytoskeleton (C)-enriched subcellular fractions. MHCIIA levels were reduced in the non-cytoskeleton fraction in TNFα-treated cells and the levels recovered after blocking caspase activity (Fig. 3A, N-labelled lanes in MHCIIA blot). MHCIIA content in the cytoskeleton-enriched fraction was decreased separately by Z-VAD-fmk and TNFα when compared with control levels (Fig. 3A, C-labelled lanes in MHCIIA blot). Treatment of TtT/GF cells with TNFα in combination with Z-VAD-fmk increased MHCIIA levels in the cytoskeleton fractions with respect to those measured in cells treated with TNFα alone. However, MHCIIA levels were lower than those found in Z-VAD-fmk-treated or control cells (Fig. 3A, C-labelled lanes in MHCIIA blot). Two different polyclonal MHCIIA antibodies yielded the same result. No MHCIIA fragments were detected by these antibodies in any of the subcellular factions. The effect of TNFα on MHCIIB was very different. Cytoskeleton-associated MHCIIB was not affected by TNFα treatment, whereas non-cytoskeleton-MHCIIB was slightly reduced by the treatment

and this reduction was abolished by the caspase inhibitor (Fig. 3A, MHCIIB). Similar results were obtained with three different antibodies against MHCIIB.

These results demonstrate that TNFα alone is capable of inducing TtT/GF cell apoptosis when the cells are incubated for long periods of time. Probably, the delay in inducing apoptosis is because TNFα elicits both anti-apoptotic and pro-apoptotic signals, but with time the apoptotic signals prevail in TtT/GF cells. To block the TNFα-induced anti-apoptotic signals, we inhibited the survival pathways using the eukaryotic protein synthesis inhibitor cycloheximide (CHX, 5 μg/ml). In addition, to assess whether the different behaviour of the two myosin II isoforms also takes place in other cells, we also used NIH 3T3 fibroblasts. A 24 hours-incubation with either TNFα or CHX did not affect MHCIIA levels; however, TNFα together with CHX reduced MHCIIA levels which were restored by Z-VADfmk in both cell types (Fig. 3B). On the contrary, MHCIIB levels in TtT/GF cells were not affected by neither TNFα nor CHX nor a combination of the compounds (Fig. 3B). TNFα alone did not affect MHCIIB but together with CHX slightly decreased the levels of the protein in NIH 3T3 fibroblasts (Fig. 3B).

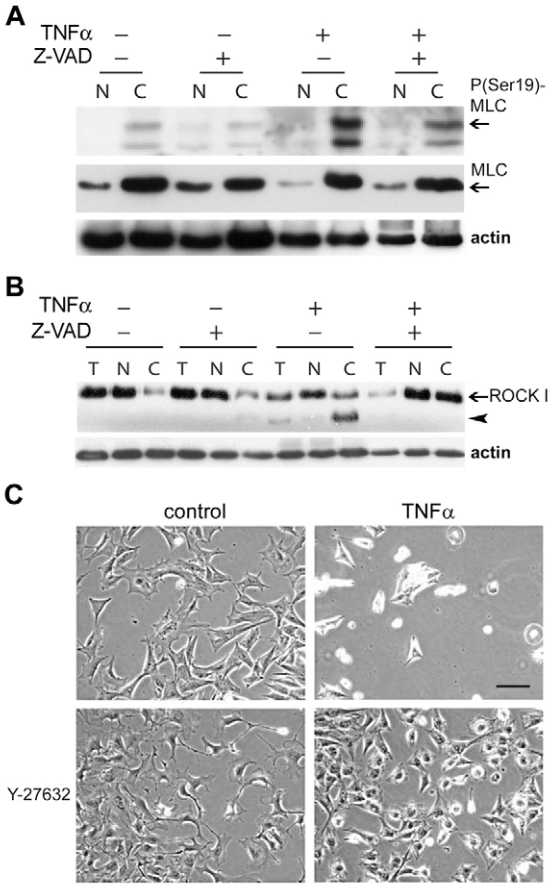

Fig. 2. Effect of long-term TNFα treatment on MLC phosphorylation state in TtT/GF cells. TtT/GF cells were incubated with medium alone or with medium containing 20 ng/ml TNFα for 96 hours. Following the treatments, cells were scraped off and total-cell lysate (T), non-cytoskeleton (N) and cytoskeleton (C) fractions were prepared and subjected to electrophoresis and western blotting with different antibodies. (A) Specific antibody against MLC phosphorylated at Ser19 [labelled P-(Ser19)-MLC] detected phosphorylated MLC in the cytoskeleton-enriched (C) fraction of control and treated cells. TNFα increased MLC-Ser19-*P* levels. The increase was blocked by the caspase inhibitor Z-VADfmk. The same membrane was stripped and reprobed for MLC. Most MLC (arrow) was recovered in the cytoskeleton fraction. Cytoskeleton-associated MLC was slightly increased by TNFα, whereas non-cytoskeleton-associated MLC decreased in TNFα-treated cells. The decrease was partly abolished by the caspase inhibitor Z-VAD-fmk. The actin immunoreactive bands correspond to the loading control. (B) Incubation of TtT/GF cells with TNFα for 96 hours induced ROCK1 cleavage and translocation to the cytoskeleton fraction of the full-length enzyme. Cleaved, active ROCK1 was recovered in the cytoskeleton-enriched fraction (arrowhead). The caspase inhibitor Z-VAD-fmk blocked TNFα-induced ROCK1 cleavage. The actin immunoreactive bands correspond to the loading controls. (C) Representative phase-contrast micrographs of TtT/GF cells incubated with culture medium alone or with medium containing TNFα both in the absence (control) or presence of the ROCK inhibitor Y-27632 (5 μM). ROCK inhibition in control cells caused cell-body retraction and increased lamellipodia and cellular processes. TNFα-induced cell shrinkage and detachment were abolished by Y-27632. Scale bar: 100 μm.

To characterise the differential stability of MHCII isoforms A and B, TtT/GF cells were incubated with the protein synthesis inhibitor CHX (50 μg/ml; Fig. 3C) or with the transcription inhibitor actinomycin D (ActD, 1 μg/ml; Fig. 3D) for increasing periods of time. The expression levels of each myosin II isoform was assessed by western blotting. The MHCIIA protein and mRNA showed a faster turnover than those of MHCIIB.

MHCIIB$^{-/-}$ embryonic fibroblasts

Our results show that MHCIIB was less affected than MHCIIA during cytoskeleton reorganisation in cells undergoing apoptosis. Perhaps, MHCIIB is the isoform that remains longer in the cells, to form the active actomyosin fibers that mediate some morphological responses during the execution phase of the apoptotic process. This was investigated by using a stable mouse embryonic cell line lacking MHCIIB (MHCIIB$^{-/-}$ fibroblasts) with the corresponding wild-type cells (Tullio et al., 1997). The MHCIIB$^{-/-}$ fibroblasts express neither MHCIIB nor MHCIIC but only MHCIIA (Lo et al., 2004), which is therefore the only MHCII isoform to interact with MLC and to be incorporated in the actomyosin contractile fibers in these cells.

The wild-type and MHCIIB$^{-/-}$ fibroblasts were treated with culture medium alone, or with culture medium containing either TNFα or TNFα plus CHX for 24 hours. Short-term incubation with TNFα did not affect MHCIIA levels in either wild-type or MHCIIB$^{-/-}$ fibroblasts (Fig. 4A,B). However, TNFα together with CHX decreased MHCIIA levels in both cell lines (Fig. 4A,B). The effect was blocked by the caspase inhibitor Z-VAD but not by ROCK inhibitor Y-27632 (Fig. 4A,B). MHCIIB levels were not affected by any of those treatments in the wild-type fibroblasts (Fig. 4A). Spectrin cleavage was similar in both wild-type and MHCIIB$^{-/-}$ embryonic fibroblasts (Fig. 4A), indicating that other members of the actin cytoskeleton were similarly affected in wild-type and MHCIIB$^{-/-}$ cells. Indeed, caspase 3 was processed similarly in wild-type and MHCIIB$^{-/-}$ fibroblasts (Fig. 4A). Furthermore, a time-course study revealed that wild-type and MHCIIB$^{-/-}$ embryonic fibroblasts responded to TNFα+CHX treatment by activating caspase 3 and by degrading MHCIIA with similar kinetics (Fig. 5A). In addition, there was no difference in the percentage of active caspase-3-positive cells during TNFα+CHX treatment in both cell lines, indicating that the absence of MHCIIB did not affect the rate of cell death (Fig. 5B).

We next evaluated whether the morphological responses that normally take place in cells undergoing apoptosis were affected or not by the absence of MHCIIB. Wild-type embryonic fibroblasts treated with TNFα+CHX retracted and detached (Fig. 6A). By contrast, most MHCIIB$^{-/-}$ fibroblasts subjected to the same

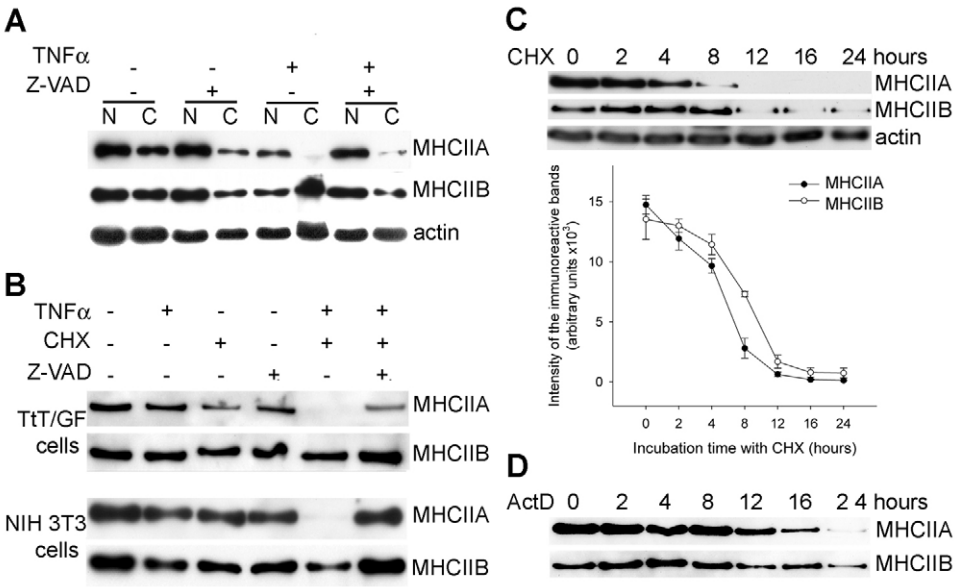

Fig. 3. TNFα treatment decreased MHCIIA levels but did not affect MHCIIB levels. (A) TtT/GF cells were treated with culture medium alone or with medium containing 20 ng/ml TNFα both in the absence or in the presence of 5 μM Z-VAD-fmk for 96 hours. Next, non-cytoskeleton (N) and cytoskeleton (C) fractions were obtained and subjected to electrophoresis and western blotting with antibodies against MHCIIA. The membrane was then stripped and reprobed with anti-MHCIIB. The actin immunoreactive bands correspond to the loading control. Z-VAD-fmk slightly decreased MHCIIA levels in the cytoskeleton fraction. TNFα reduced MHCIIA levels in both subcellular fractions. Inhibition of caspase activity restored control non-cytoskeleton MHCIIA levels but the recovery was not complete in the cytoskeleton fraction. MHCIIB levels in the cytoskeleton fraction were slightly decreased by Z-VAD-fmk but were not affected by TNFα. (B) TtT/GF and NIH 3T3 cells were treated with different combinations of TNFα (20 ng/ml), cycloheximide (CHX, 5 μg/ml) and Z-VAD-fmk (5 μM). Following a 24-hour treatment, MHCIIA and MHCIIB expression levels were analysed by western blotting in whole-cell lysates. Short-term incubation of the two cell lines with TNFα in combination with CHX drastically reduced MHCIIA, whereas MHCIIB expression remained almost unchanged in TtT/GF cells and was slightly reduced in NIH 3T3 fibroblasts. The TNFα+CHX-induced drop of MHCIIA levels was abolished by the caspase inhibitor Z-VAD-fmk in both cell lines. (C) TtT/GF cells were incubated with the protein synthesis inhibitor cycloheximide (CHX, 50 μg/ml) for increasing periods of time. Following treatments, total cell proteins were subjected to SDS-PAGE followed by immunoblotting with anti-MHCIIA. Next, the membrane was stripped and incubated with anti-MHCIIB. The actin immunoreactive bands correspond to the loading control. The figure shows representative immunoblots. The bands were scanned and the mean intensity values for each myosin isoform were plotted. Values shown are the mean ± s.e.m. of three independent experiments. (D) TtT/GF cells were incubated with the translation inhibitor actinomycin D (ActD, 1 μg/ml) for increasing periods of time. Blockade of protein or mRNA synthesis affected MHCIIA more rapidly than MHCIIB.

treatment remained flat and adherent (Fig. 6A). Quantification of cell attachment demonstrated a tenfold increase in the number of attached cells in the MHCIIB$^{-/-}$ cell line with respect to wild-type fibroblasts after TNFα+CHX treatment (Fig. 6B). The percentage of apoptotic cells, i.e. cells labelled with active caspase 3 that remained flat and adherent during TNFα+CHX treatment, was also higher within the MHCIIB$^{-/-}$ than within the wild-type fibroblasts from 16 hours onwards (Fig. 6C). Since we have shown that the percentage of apoptotic cells for each time point is similar in both cell lines (Fig. 5B), this result indicates that there is an accumulation of flat cells within the apoptotic MHCIIB$^{-/-}$ cell population.

We further characterised this differential behaviour by double labelling the TtT/GF cells and the wild-type and MHCIIB$^{-/-}$ embryonic fibroblasts with Rhodamine-phalloidin to exhibit the filamentous actin (F-actin) distribution, and with antibody against active caspase 3 to label the apoptotic cells (Fig. 7). All control cells were flat and showed plasma membrane projections, and cortical and cytoplasmic F-actin (Fig. 7, control, F-actin). As expected, the control cells displayed a low level of caspase 3 activation (Fig. 7, control, active caspase 3). Following TNFα+CHX treatment for 16 hours, most TtT/GF cells and wild-type fibroblasts that remained adherent and showed labelling for active caspase 3 were retracted (Fig. 7, TNFα+CHX-treated TtT/GF and wild-type cells). Note that caspase 3 was not activated in TNFα+CHX-treated TtT/GF cells that stayed flat (Fig. 7, TNFα+CHX, TtT/GF cells, arrows). However, most TNFα+CHX-treated MHCIIB$^{-/-}$ fibroblasts that remained flat and adherent showed actin filaments and activation of caspase 3 (Fig. 7, TNFα+CHX, MHCIIB$^{-/-}$ fibroblasts, see also supplementary material Fig. S1). In these cells, active caspase 3 was distributed as cytoplasmic dots (Fig. 7, MHCIIB$^{-/-}$ fibroblasts).

Participation of PKCζ in TNFα-induced morphological responses during apoptosis

Having established the importance of MHCIIB in cell shrinkage during apoptosis, we further analysed the mechanisms by which MHCIIB mediates cell contraction. Recent reports have shown that MHCIIB, but not MHCIIA, is rapidly phosphorylated following EGF stimulation by a complex involving PAK1 and the atypical PKC isoform ζ (Even-Faitelson and Ravid, 2006). PKCζ is activated by phosphorylation at threonine residue 140 (Thr410) (Smith et al., 2003) and by a caspase-mediated cleavage that releases the C-terminal catalytic domain from the N-terminal autoinhibitory domain (Smith et al., 2000). We investigated whether PKCζ is involved in MHIIB-mediated cell rounding up and detachment during apoptosis. TNFα+CHX treatment of TtT/GF cells caused the cleavage of endogenous PKCζ with a time course similar to that of caspase 3 cleavage (Fig. 8A). The PKCζ fragment was recovered in the cytoskeleton-enriched fraction (Fig. 8B). TNFα+CHX also induced the translocation of full-length PKCζ to

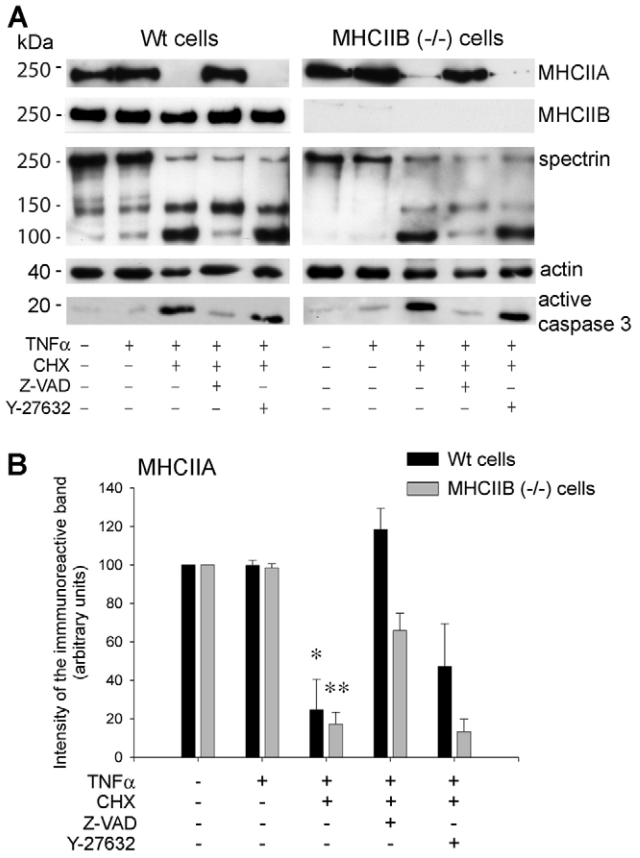

Fig. 4. Effect of TNFα+CHX treatment on MHCIIA and MHCIIB levels in wild-type and MHCIIB$^{-/-}$ embryonic fibroblasts. (A) Wild-type and MHCIIB$^{-/-}$ embryonic fibroblasts were treated with different combinations of TNFα (20 ng/ml), CHX (5 μg/ml), Z-VAD-fmk (5 μM) and Y-27632 (20 μM) for 24 hours. Following treatments, total cell lysates were subjected to western blotting with antibodies against MHCIIA, MHCIIB, spectrin, actin and active caspase 3. TNFα+CHX treatment reduced MHCIIA levels and caused the cleavage of spectrin and caspase 3 in both wild-type and MHCIIB$^{-/-}$ cells. Control conditions for each protein were restored by the caspase inhibitor Z-VAD-fmk but not by Y-27632. MHCIIB expression in wild-type cells was not affected by the treatments. The figure shows representative western blots. (B) Quantification of MHCIIA levels in wild type and MHCIIB$^{-/-}$ fibroblasts. The intensity of the MHCIIA immunoreactive bands was measured for each experimental condition described in A and normalised to control cell levels. Values shown are the mean ± s.e.m. of three independent experiments. The graph shows that TNFα+CHX treatment had a similar effect on MHCIIA levels in both cell lines. *P<0.01: wild-type fibroblasts, TNFα vs TNFα+CHX; **P<0.0002: MHCIIB$^{-/-}$ fibroblasts, TNFα vs TNFα+CHX.

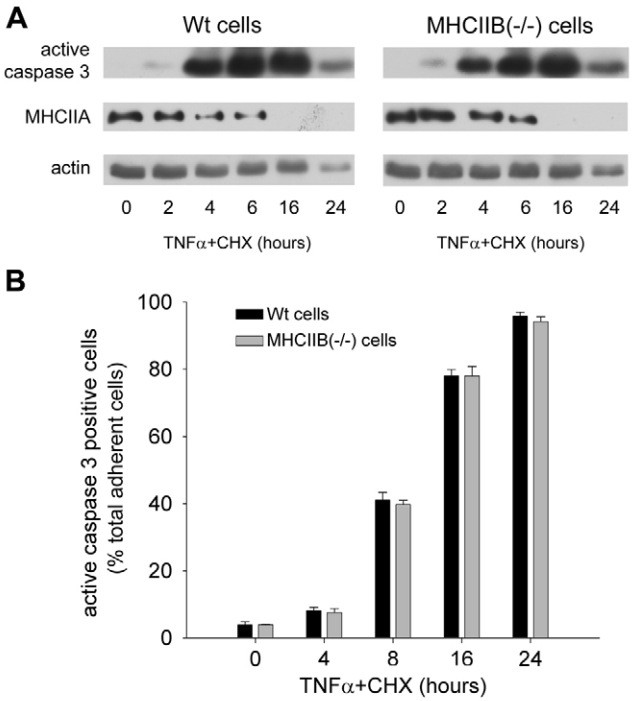

Fig. 5. Time course studies on the effect of TNFα+CHX treatment on caspase 3 activation and MHCIIA degradation in wild type and MHCIIB$^{-/-}$ embryonic fibroblasts. Wild type and MHCIIB$^{-/-}$ cells were incubated in the absence (0 hour) or in the presence of TNFα+CHX for increasing periods of time (2-24 hours). (A) Total cell lysates were subjected to western blotting analyses: the same membrane was incubated with antibodies against active caspase 3, MHCIIA and actin. The figure shows representative western blots. The time course of caspase 3 cleavage and of MHCIIA disappearance was similar in the two cell lines. (B) Following treatments, cells were processed for immunofluorescence microscopy with anti-active caspase 3 and Rhodamine-phalloidin. Total adherent cells and adherent cells positive for active caspase 3 were counted for each time point. TNFα+CHX treatment induced an increase in the percentage of cells positive for active caspase 3 with the same time course in both cell lines. The values shown are the mean ± s.e.m. of three independent experiments and more than 300 cells were observed per experimental condition.

the cytoskeleton fraction (Fig. 8B). PKCζ cleavage but not its translocation to the cytoskeleton was blocked by caspase inhibition (Fig. 8B). PKCζ cleavage following TNFα+CHX treatment also took place in NIH 3T3 fibroblasts, wild-type and MHCIIB$^{-/-}$ embryonic fibroblasts although with different kinetics (Fig. 8C).

PKCζ and MHCIIB have been demonstrated to physically interact (Even-Faitelson and Ravid, 2006). Here, we show that PKCζ and MHCIIB co-immunoprecipitated in untreated TtT/GF cells (Fig. 9A,B) as well as in TtT/GF cells treated with TNFα+CHX (Fig. 9C). To evaluate the involvement of PKCζ in TNFα+CHX-induced cell retraction during apoptosis, TtT/GF cells and wild-type and MHCIIB$^{-/-}$ embryonic fibroblasts were treated with the specific PKCζ inhibitor Myr-PKCζ pseudosubstrate for 16 hours. Inhibition of PKCζ activity in control cells induced the formation of cytoplasmic projections but the cells remained adherent (Fig. 10). Myr-PKCζ pseudosubstrate neither induced the apoptosis of any of the cells examined (Fig. 10) nor inhibited TNFα-induced cleavage of caspase 3 (supplementary material Fig. S2). However, PKCζ inactivation reduced TNFα+CHX-induced cell retraction in TtT/GF cells and wild-type embryonic fibroblasts (Fig. 10) but was without effect on TNFα+CHX-treated MHCIIB$^{-/-}$ cells (Fig. 10).

Discussion

The study provides evidence of a distinctive role of MHCIIA and MHCIIB isoforms during the execution phase of apoptosis. We demonstrate that MHCIIB, together with the phosphorylated MLCs and actin, is required for the assembly of a functional contractile cytoskeleton involved in the retraction and detachment of cells undergoing apoptosis. In addition, we show that PKCζ has a facilitatory role in this process. Because TNFα elicits both apoptotic and antiapoptotic signals (Baud and Karin, 2001), it is not considered a good apoptotic inducer and, therefore, it is used in combination with a protein synthesis inhibitor to selectively trigger the apoptotic

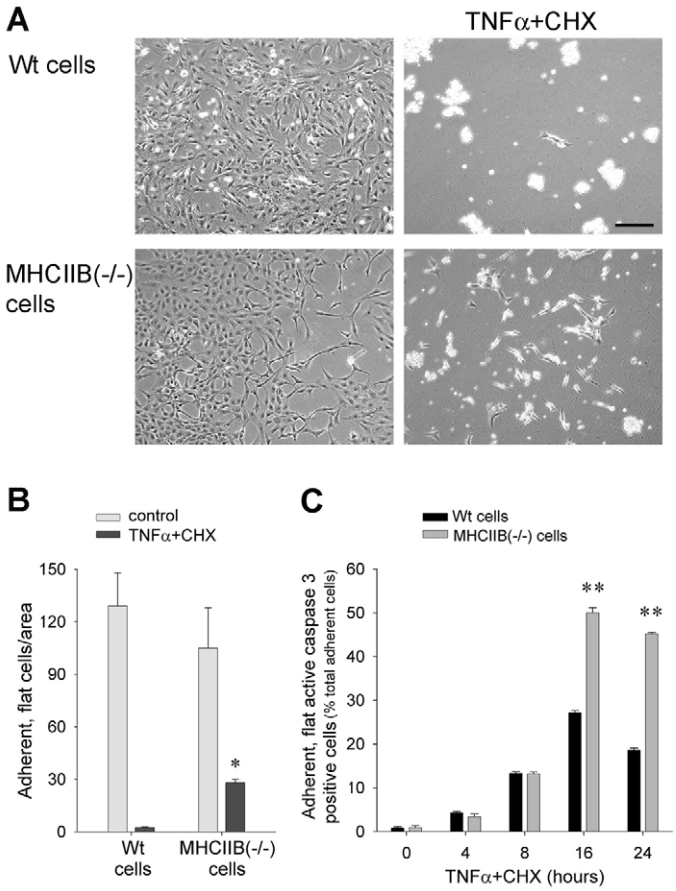

Fig. 6. Differential morphological responses of wild-type and MHCIIB$^{-/-}$ embryonic fibroblasts during TNFα+CHX-induced apoptosis. Wild-type and MHCIIB$^{-/-}$ cells were incubated in the absence (control) or in the presence of TNFα+CHX for 24 hours. (A) Representative bright-field micrographs of control and treated cells. TNFα+CHX induced cell the shrinkage and detachment of wild-type and MHCIIB$^{-/-}$ embryonic fibroblasts; however, more MHCIIB$^{-/-}$ than wild type cells remained attached. Scale bar: 250 μm. (B) Adherent cells in ten different areas per experimental condition were counted. Quantification of the responses demonstrated a larger number of adherent MHCIIB$^{-/-}$ than wild-type cells after the treatment. Data shown are the mean ± s.e.m. of six independent experiments. *P<0.0001, treated MHCIIB$^{-/-}$ vs treated wild-type fibroblasts. (C) Wild-type and MHCIIB$^{-/-}$ embryonic fibroblasts were incubated for increasing periods of time with TNFα+CHX. Following treatments, the cells were processed for immunofluorescence microscopy with anti-active caspase 3 to identify the apoptotic cells and with Rhodamine-phalloidin to facilitate cell visualisation. Adherent, flat cells that were positive for active caspase 3 were counted and the percentage of these cells with respect to the total adherent cell population was calculated. The percentage of apoptotic cells that were flat and adherent was higher in MHCIIB$^{-/-}$ than in wild-type fibroblasts from 16 hours onwards. More than 300 cells per experimental condition were counted. The values shown are the mean ± s.e.m. of three independent experiments. **P<0.00001, wild-type cells vs MHCIIB$^{-/-}$ cells 16 and 24 hours treatment.

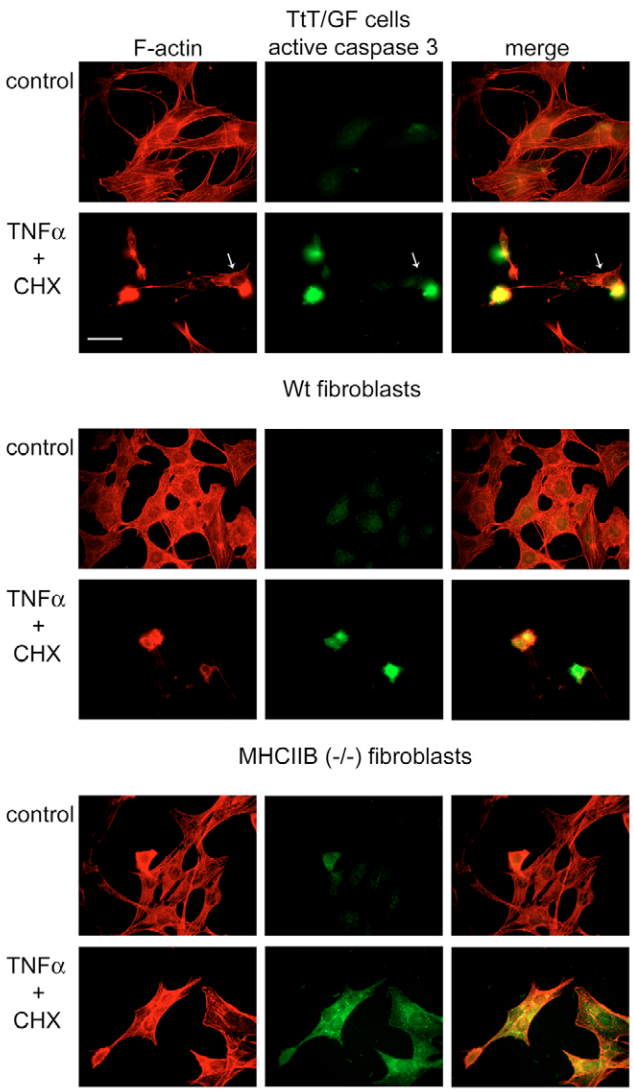

Fig. 7. Fluorescence microscopy of F-actin distribution and caspase 3 activation in control and TNFα+CHX-treated TtT/GF cells, and wild-type and MHCIIB$^{-/-}$ embryonic fibroblasts. The cells were incubated with culture medium alone (control) or containing TNFα+CHX for 16 hours. Next, the cells were processed for fluorescence microscopy with Rhodamine-phalloidin and anti-active caspase 3. Control cells were flat and showed cytoplasmic extensions and cortical and cytoplasmic actin filaments. Control cells showed low levels of caspase 3 activation. Following TNFα+CHX treatment, the few TtT/GF cells and wild-type fibroblasts that remained attached were round and displayed caspase 3 activation. Some treated TtT/GF cells that remained flat showed no evidence of caspase 3 activation (arrows). Treated MHCIIB$^{-/-}$ cells that remained attached were flat and possessed actin fibers. Moreover, caspase 3 was active in these adherent, TNFα+CHX-treated MHCIIB$^{-/-}$ cells. Scale bar: 50 μm.

pathway. However, we found that long-term TNFα treatment induced biochemical and morphological features in TtT/GF cells that are typical to cells undergoing apoptosis (Earnshaw, 1995; Mills et al., 1999). Furthermore, the morphological and biochemical responses observed in cells treated with TNFα either alone or in combination with CHX were similar, except that all events occurred faster in the presence of CHX.

The morphological responses taking place during the execution stage of the apoptotic process require the participation of the actin cytoskeleton (Coleman and Olson, 2002). Proteolysis of several actin-binding proteins contributes to cell shrinkage and detachment (Brancolini et al., 1997; Chen et al., 2001; Jänicke et al., 1998; Kook et al., 2003). At the same time, a contractile actomyosin system is necessary for cell contraction, apoptotic body formation and nuclear breakdown (Croft et al., 2005; Lane et al., 2005; Mills et al., 1998). A paradox seems to underlie this experimental evidence: a dismantling yet functional actin cytoskeleton is needed for a successful execution phase.

The involvement of MLC phosphorylation in the regulation of actomyosin contraction during apoptosis is well established; however, the implication of the MHCIIs in the apoptotic process is not. We show here, for the first time, a distinct contribution of MHCII isoforms A and B to the apoptotic process: MHCIIB levels remained unchanged, whereas those of MHCIIA decreased significantly during TNFα or TNFα+CHX treatment in TtT/GF cells, NIH 3T3 fibroblasts and embryonic fibroblasts. MHCIIA cleavage has already been recorded in TNFα+CHX-treated aortic endothelial cells (Suarez-Huerta et al., 2000a) and anti-Fas-treated Jurkat cells (Gerner et al., 2000; Kato et al., 2005). Surprisingly, MHCIIA cleavage products were either not recognised by the antibodies used (Suarez-Huerta et al., 2000a) or their recognition was due to a crossreactivity with another antibody (Kato et al., 2005). The two different MHCIIA antibodies used in the present study also failed to detect any MHCIIA fragment.

Since we found that MHCIIA has a faster turnover than MHCIIB, low MHCIIA levels in TNFα+CHX-treated cells may be the result of the rapid disappearance of MHCIIA following protein synthesis inhibition. However, the same downregulation of MHCIIA but not of MHCIIB was obtained in long-term TNFα-treated cells in which protein synthesis was not exogenously inhibited. In addition, MHCIIA possesses consensus sequences for caspase 3 proteolysis (Kato et al., 2005); therefore, by default, it is broken down during the execution phase of the apoptotic process. In accordance with this, reduced MHCIIA levels in apoptotic cells were restored to control values by inhibiting caspase activity (Gerner et al., 2000; Suarez-Huerta et al., 2000a) (and this paper). Therefore, the experimental data indicate that the loss of MHCIIA and the conservation of MHCIIB are specific events of the apoptotic process not a consequence of a different stability of the isoforms.

But why then is the isoform A lost but the isoform B retained? On the one hand, experimental evidence has demonstrated the need of actin contractile fibers for cell contraction and detachment during apoptosis. Our results suggest that there is a specific dismantling of actomyosin fibers made of MHCIIA during apoptosis. The observation of MHCIIA in late blebs together with the phosphorylated MLCs (Lane et al., 2005) agrees with this idea. On

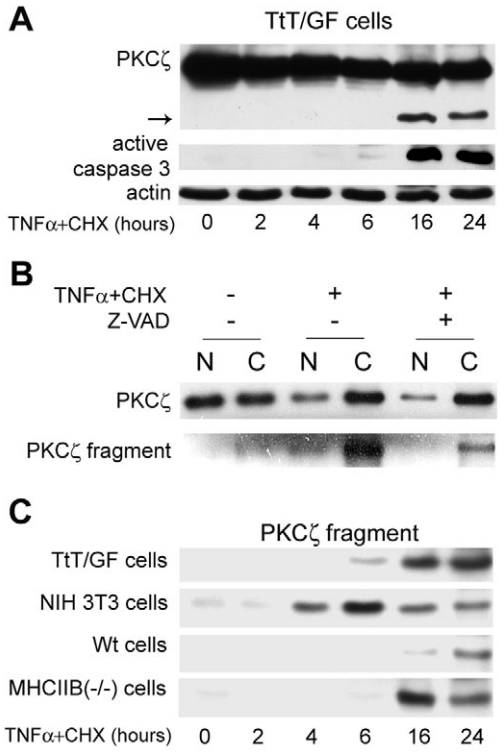

Fig. 8. Effect of TNFα+CHX on PKCζ cleavage. (A) TtT/GF cells were incubated with TNFα+ CHX for increasing periods of time. Next, total cell lysates were prepared and subjected to western blotting with antibodies to PKCζ and active caspase 3. The membrane was striped and incubated with anti-actin as loading control. The representative western blots shows PKCζ cleavage in cell incubated with TNFα+CHX for more than 16 hours. The cleavage was coincident with caspase 3 activation. (B) TtT/GF cells were incubated culture medium alone or containing TNFα+CHX either in the absence or presence of the caspase inhibitor Z-VAD-fmk for 16 hours. Next, the cells were homogenised and non-cytoskeleton (N)- and cytoskeleton (C)-enriched fractions were prepared. The subcellular fractions were subjected to western blot analyses with anti-PKCζ. The figure shows representative western blots. PKCζ is present in both subcellular fractions in control and treated cells. TNFα+CHX treatment induced the translocation of PKCζ from the non-cytoskeleton (N) to the cytoskeleton (C) fraction. The PKCζ cleavage product was only found in the cytoskeleton (C)fraction of TNFα+CHX-treated cells. The caspase inhibitor Z-VAD-fmk blocked TNFα+CHX- induced PKCζ cleavage but not its translocation. (C) TtT/GF cells, NIH 3T3 fibroblasts, wild-type and MHCIIB$^{-/-}$ embryonic fibroblasts were treated with TNFα+CHX for increasing periods of time. Next, cell lysates were prepared and 10 μg protein per sample were subjected to electrophoresis and western blotting with anti-PKCζ. The representative western blots show the appearance of a 48 kDa immunoreactive band that corresponds to one of the cleavage products of PKCζ after TNFα+CHX treatment in all cell lines.

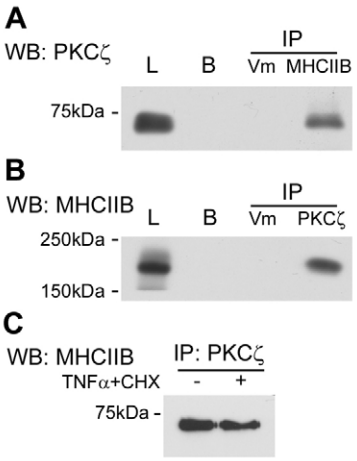

Fig. 9. Co-immunoprecipitation studies on the effect of TNFα+CHX on PKCζ-MHCIIB interaction. (A) TtT/GF cell lysates were prepared from untreated cells (L). Precleared cell lysates were incubated with proteinA-Sepharose4B beads that had been preincubated with either buffer alone (B) or anti-vimentin (Vm) or anti-MHCIIB (MHCIIB). The pellets were subjected to SDS-PAGE followed by immunoblotting with anti-PKCζ antibody. A representative membrane shows the presence of a 70 kDa immunoreactive band in the cell lysate and in the MHCIIB immunoprecipitate. (B) Untreated TtT/GF cell lysates (L) were prepared. Precleared cell lysates were incubated with proteinA-Sepharose4B beads that had been preincubated with either buffer alone (B), anti-vimentin (Vm) or anti-PKCζ (PKCζ) antibodies. The pellets were subjected to SDS-PAGE followed by immunoblotting with anti-MHCIIB. A representative membrane shows the presence of a 210 kDa immunoreactive band in the cell lysate and in the PKCζ immunoprecipitate. (C) Control and TtT/GF cells treated for 24 hours with TNFα+CHX were subjected to immunoprecipitation with PKCζ antibody. The pellets were recovered and subjected to western blotting with MHCIIB antibodies. This representative membrane shows presence of a 70 kDa immunoreactive band in the immunoprecipitates of both untreated and treated cells.

the other hand, MHCIIB and actin were virtually not affected by TNFα. MHCIIB was reported to bind to actin more slowly and weakly than MHCIIA (Bresnick, 1999; Kolega, 2003; Kolega, 2006). Thus, MHCIIA proteolysis could facilitate the access of MHCIIB molecules to the actin fibers due to a lack of competition with MHCIIA. In support of this view is the report that MHCIIB but not MHCIIC is assembled into cytoplasmic stress fibers in the absence of MHCIIA (Bao et al., 2005). Therefore, MHCIIB may be the main contributor to actomyosin fibers in apoptotic cells.

MHCIIA is responsible for the forward movement of the cell body during locomotion, whereas MHCIIB is responsible for cell retraction and remains associated with stable stress fibers (Kolega, 2003). We have shown that increased association of myosin II with cortical actin participates in the rounding-up of cells (Vitale and Carbajal, 2004). Disposal of MHCIIA and maintenance of MHCIIB in the apoptotic cells would shift the locomotion and contraction balance towards cell contraction. Our observation of a larger number of flat and adherent apoptotic MHCIIB$^{-/-}$ fibroblasts than apoptotic wild-type fibroblasts during TNFα treatment, supports the view of a requirement of MHCIIB for actomyosin fiber assembly necessary for cell contraction during apoptosis. The fact that COS-7 cells, which lack MHCIIA, contract and detach during apoptosis adds supports to the notion (Orlando et al., 2006). However, the removal of MHCIIA and, therefore, the disassembly of actin-MHCIIA fibers probably contribute to the dismantling of focal adhesions that is also required for detachment. Instability of MHCIIA affects focal adhesions (Dulyaninova et al., 2007).

The contribution of MHCII phosphorylation in the stability of myosin fibers has become increasingly manifest (Even-Faitelson and Ravid, 2006; Murakami et al., 2000; Straussman et al., 2001). Once again, the kinetics of the phosphorylation and the kinases involved differ for the A and B isoforms (Dulyaninova et al., 2007; Kolega, 1999; Redowicz, 2001). Among the several kinases that phosphorylate the MHCIIs, the atypical PKC isoform ζ is of particular significance because, on the one hand, this kinase interacts and phosphorylates MHCIIB not MHCIIA (Even-Faitelson and Ravid, 2006) and, on the other hand, PKCζ is itself a target of caspase 3 (Smith et al., 2003). PKCζ activity is stimulated by phosphorylation in Thr 410, and this phosphorylation normally occurs in serum cultured cells (Smith et al., 2003). However, full activation of the enzyme is achieved by the caspase-mediated cleavage that releases the C-terminal catalytic domain from the N-terminal autoinhibitory domain (Smith et al., 2000). Under our experimental conditions, only a small proportion of total PKCζ was found cleaved by TNFα+CHX treatment. Nonetheless, because cleaved PKCζ has a shorter half-life than that of the full-length kinase (Smith et al., 2000; Smith et al., 2003), once the fragment is formed it is expected to be quickly degraded, hence reducing the intensity of the immunoreactive band.

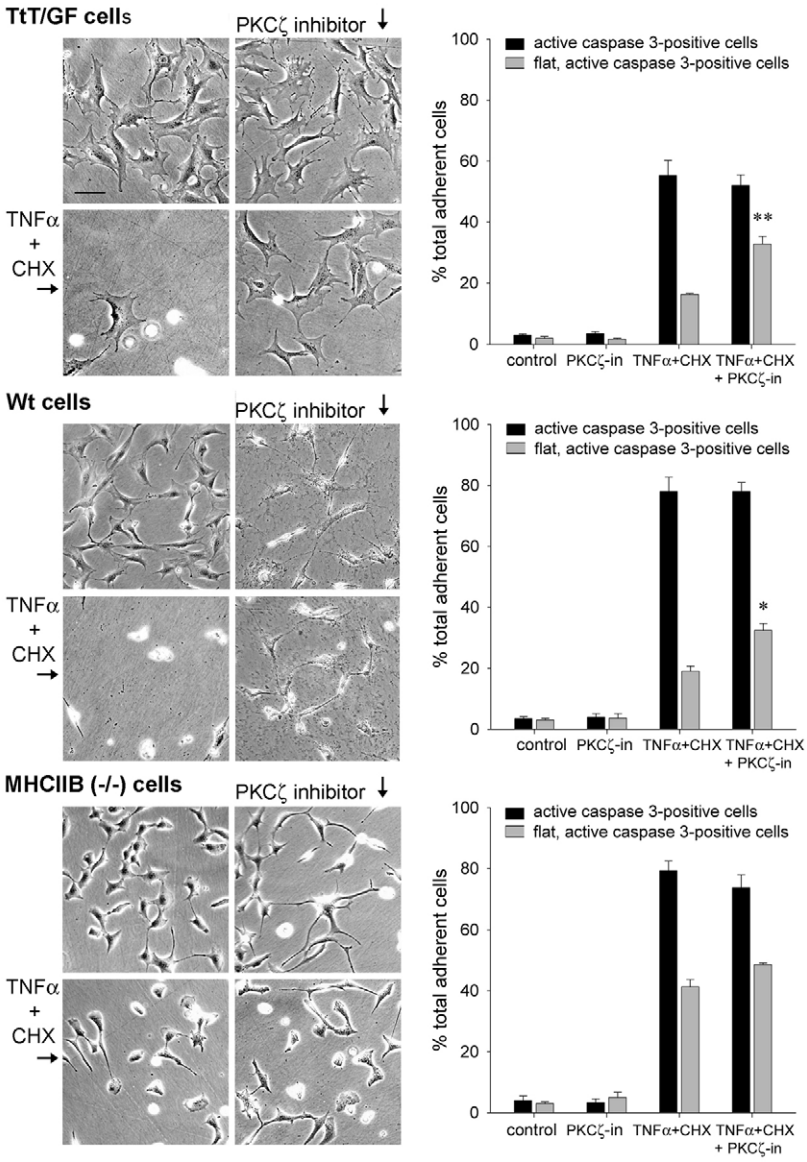

Fig. 10. Effect of PKCζ inhibition on TNFα+CHX-induced cell shrinkage and detachment. TtT/GF cells, wild-type and MHCIIB$^{-/-}$ embryonic fibroblasts were incubated with culture medium either alone or with medium containing TNFα+CHX both in the absence or presence of the specific PKCζ inhibitor Myr-PKCζ pseudosubstrate (10 μM, final concentration) for 16 hours. Some cell preparations were double labelled with anti-active caspase 3 to identify apoptotic cells and with Rhodamine-phalloidin to label F-actin. Next, the total numbers of adherent cells, of flat cells positive for active caspase 3 cells, and cells positive for active caspase 3 cells were recorded for each experimental condition. The representative phase-contrast micrographs on the left of the figure show flat and elongated control TtT/GF, wild-type and MHCIIB$^{-/-}$ cells. PKCζ-inhibited cells remained attached and showed elongated cytoplasmic processes. TNFα+CHX treatment induced cell shrinkage and detachment in TtT/GF cells and wild-type fibroblasts, but MHCIIB$^{-/-}$ cells stayed adherent and elongated. PKCζ inhibition reduced TtT/GF cell and wild-type embryonic fibroblast detachment induced by TNFα+CHX. Scale bar, 100 μm. The histograms on the right of the figure show the quantification of these results. PKCζ inhibition did not affect cell-death rate in any of the cell lines tested; however, it increased the percentage of flat apoptotic TtT/GF cells and wild-type fibroblasts but was without effect on MHCIIB$^{-/-}$ fibroblasts. The values shown are the mean ± s.e.m. of three independent experiments; more than 300 cells per experimental condition were counted. *P<0.03: TNFα+CHX+PKCζ- vs TNFα+CHX-treated wild-type fibroblasts; **P<0.005: TNFα+CHX+PKCζ- vs TNFα+CHX-treated TtT/GF cells.

Our findings that, (1) PKCζ and MHCIIB physically interacted not only in control cells but in TNFα-treated cells as well, (2) TNFα induced the translocation of PKCζ to the cytoskeleton and, (3) cleaved PKCζ was associated with the cytoskeleton fraction, provide strong support to the idea that MHCIIB is a target of PKCζ during TNFα-induced apoptosis. Specific inhibition of PKCζ did not induce cell death and did not affect TNFα-induced caspase 3 processing. However, PKCζ inactivation blocked TNFα-induced retraction and detachment of TtT/GF cells and of wild-type embryonic fibroblasts, indicating that the activity of the kinase is necessary for actin cytoskeleton remodelling in apoptotic cells. The fact that TNFα-induced morphological responses were less affected by PKCζ inhibition in MHCIIB$^{-/-}$ fibroblasts than in the cells expressing MHCIIB suggests that PKCζ-MHCIIB interaction plays an important role in TNFα-induced cell contraction during apoptosis.

Besides MHCIIB contribution, our results confirm the implication of ROCK1-mediated MLC phosphorylation in cell contraction and detachment during the execution phase of apoptosis. Moreover, our findings extended previous observations by showing that cleaved, activated ROCK1 and phosphorylated MLC were both specifically associated with the cytoskeleton fraction. The results highlight the fact that TNFα induced the translocation of some cytoskeleton-related proteins (such as MLC, ROCK1 and PKCζ) from the non-cytoskeleton to the cytoskeleton fraction, and that this effect was independent of caspase activation.

Together, our results indicate that, during the execution phase of apoptosis, there is an increased detachment of actin fibers to the cell periphery (downregulation or cleavage of MHCIIA, α-actinin and spectrin) accompanied by a reinforcement of the actin-MHCIIB contractile fibers (increased cytoskeleton association or activation of ROCK1, phosphorylated MLC, MHCIIB and actin). These results may explain the apparent paradox of a dismantling yet functional actin cytoskeleton.

Materials and Methods

Cell culture

The folliculostellate cell line TtT/GF was obtained from U. Renner (Department of Endocrinology, Max Planck Institute of Psychiatry, Munich, Germany). The MHCIIB$^{-/-}$ cells and control mouse embryonic fibroblasts were obtained from R. S. Adelstein (Laboratory of Molecular Cardiology, National Heart, Lung and Blood Institute, National Institutes of Health, Bethesada, MD). All cell lines were cultured in Dulbecco's modified Eagle's medium (DMEM) supplemented with 5% of foetal bovine serum, 3.7 g/ml of $NaHCO_3$, 10 mM Hepes (pH 7.2), and antibiotics (penicillin 0.2 mg/ml and streptomycin 50 μg/ml) at 37°C in an atmosphere of 5% CO_2 and 95% air. The cells were cultured for 48 hours before subjected to different treatments.

Source of antibodies and chemicals

Several antibodies against MHC were used: rabbit polyclonal anti-MHCIIA antibody raised against a synthetic peptide corresponding to amino acids 1950-1961 of human nonmuscle MHCIIA and rabbit polyclonal anti-MHCIIB antibody raised against synthetic peptide corresponding to amino acid residues 1965-1976 of human nonmuscle MHCIIB were obtained from Sigma Chemical Co. (St Louis, MO). Rabbit polyclonal anti-MHCIIA antibody raised against a peptide with the sequence GKADGAEAKPAE corresponding to the C-terminus of human nonmuscle MHCIIA and rabbit polyclonal anti-MHCIIB antibody generated against a peptide with the sequence SDVNETQPPQSE corresponding to the C-terminus of nonmuscle MHCIIB were purchased from Convance (Berkeley, CA). Mouse monoclonal nonmuscle anti-chicken MHCIIB antibody (CMII 23) was developed by G. W. Conrad and A. H Conrad (Division of Biology, Kansas State University, Manhattan, KS) and obtained from the Developmental Studies Hybridoma Bank University of Iowa, Dept Biological Sciences developed under the auspices of the NICHD. Rabbit polyclonal antibody against activated caspase 3, raised against a synthetic peptide corresponding to the cleavage site of human caspase 3 and that only recognises the 17 kDa fragment of active caspase 3, as well as mouse monoclonal anti-MLC, rabbit polyclonal anti-actin, horseradish peroxidase (HRP)-conjugated anti-mouse IgM antibodies, proteinA Sepharose-4B, cycloheximide and actinomycin were purchased from Sigma Chemical Co. HRP-conjugated anti-mouse IgG, HRP-conjugated anti-goat IgG and HRP-conjugated anti-rabbit IgG antibodies were purchased from Jackson ImmunoResearch Laboratories (West Grove, PA). Mouse monoclonal anti-ROCK1 antibody was purchased from BD Biosciences (Mississauga, ON, Canada). Mouse monoclonal antibodies against α-actinin, non-erythroid α-spectrin and goat polyclonal anti-vimentin antibody were from Chemicon International (Temecula, CA). The rabbit anti-caspase-8 p20 (H-134) antibody, that detects both the precursor and the activated fragment, rabbit anti-PKCζ (C-20) and goat anti-PKCζ (N-17) antibodies were obtained from Santa Cruz Biotechnology (Santa Cruz, CA). Cleaved caspase 3 (Asp175) (5A1) rabbit monoclonal antibody from Cell Signaling Technology (Danvers, MA) detects endogenous levels of the large fragment (17/19 kDa) of activated caspase 3 resulting from cleavage adjacent to Asp175. This antibody does not recognise full-length caspase 3 or other cleaved caspases. It was raised against a synthetic peptide corresponding to N-terminal residues adjacent to Asp175 of human caspase-3. Antibody against MLC phosphorylated at serine residue 19 was also purchased from Cell Signaling Technology. The vybrant^{TM} apoptosis assay kit no. 5 and Rhodamine-phalloidin were purchased from Molecular Probes (Eugene, OR). Human recombinant tumour TNFα, the Cell Death Detection ELISA^{plus} and the chemiluminescence substrate Lumilight were purchased from Roche (Laval, QC, Canada). The ROCK inhibitor Y27632 and the caspase inhibitor Z-VAD-fmk were purchased from Calbiochem (San Diego, CA). The specific PKCζ inhibitor, Myr-PKCζ pseudosubstrate was from BioSource (Camarillo, CA). Proteins in the samples were measured by the Bradford dye binding assay with materials provided by Bio Rad (Mississauga, ON, Canada).

Morphological analysis

Cells were treated with different compounds according to the specific protocol. The morphology of adherent control cells and treated cells was evaluated with an inverted microscope (Leica DMRIB, Wetzlar, Germany); the images were acquired with a Retiga Ex-I camera (Q-Imaging, Burnaby, Canada) and treated with the Northern Eclipse v6 program (Empix Imaging, Mississauga, Canada). Morphological analysis of detached cells, particularly the presence of membrane blebbing, was carried out with a Zeiss Axio-Imager Z1 microscope (Zeiss, Jena, Germany). Pictures were taken with a Zeiss HrM camera (Zeiss) and processed with the Axio-Vision v 4.5 program (Zeiss).

Fluorescence microscopy

Cells were grown on glass coverslips and incubated with different compounds according to the specific protocol. Next, cells were fixed with 3.7% formaldehyde and permeabilised with 0.5% Triton X-100 in PBS (137 mM NaCl, 3 mM KCl, 8 mM Na_2HPO_4, 1.5 mM KH_2PO_4, pH 7.4). The cells were blocked with 5% skim milk in PBS. Cells were double labelled with Rhodamine-phalloidin (1:900 dilution) to show F-actin distribution and with antibody against active caspase 3 that only recognises the 17 kDa fragment active caspase 3 to mark apoptotic cells. Next, cells were incubated with anti-rabbit-IgG-FITC. Coverslips were mounted in PBS-glycerol (1:1) containing 5% 1,4 diazabiscyclo (2,2,2) octane (DABCO). Cells were viewed with a Carl Zeiss Axiophot II fluorescence microscope (Zeiss). Pictured were acquired using Northern Eclipse program.

Quantification of apoptosis

Chromatin condensation

We used the vibrant apoptosis assay kit no. 5, which detects the compacted state of the chromatin in apoptotic cells using Hoechst 33342 and propidium iodide. Hoechst 33342 is a DNA stain that possesses a blue fluorescence and is particularly bright in the condensed nuclei of apoptotic cells. Propidium iodide which is a DNA stain presenting a red fluorescence, only enters cells with compromised plasma membranes. Briefly, following treatments, cells were rinsed in PBS and incubated with a mixture of the dyes. Next, the cells were washed and fixed in 3.7% formaldehyde and observed with a Carl Zeiss Axiophot II fluorescence microscope. Nuclei of viable cells show a less bright blue fluorescence, apoptotic cells show a very bright blue fluorescence and necrotic cells show both blue and red fluorescence. The same procedure was applied to detached cells harvested in the culture medium. We did not observe necrotic cells under our experimental conditions.

Cytoplasmic nucleosome release

The Cell Death Detection ELISA^{plus}, a photometric enzyme-immunoassay that detects cytoplasmic histone-associated-DNA fragments (mono- and oligonucleosomes) was used. In short, after treatments, the cells were scraped off and recovered by centrifugation. The pellet was incubated with the lysis buffer. Twenty microlitres of cell lysate were transferred into streptavidin-coated microplates, and incubated with a mixture of anti-histone-biotin and anti-DNA-peroxidase (POD) antibodies for 2 hours. After the removal of unbound antibodies, nucleosomes were photometrically detected by measuring POD activity with ABTS [2,2-azino-di(3-ethyl-benzthiazolin-sulfonat)] as substrate. The absorbance corresponds to the enrichment of mono- and oligonucleosomes released in the cytoplasm in each experimental condition.

Counting of detached cells

Following treatments the detached cells were recovered from the medium surrounding the cultures and cells were counted using a hemocytometer.

Counting of active caspase3-positive cells

Cells cultured on glass coverslips were subjected to TNFα+CHX treatment for increasing periods of time. At the end of each incubation period the cells were processed for immunofluorescence microscopy with active caspase 3 antibody and Rhodamine-phalloidin. Cells in the preparations were visualised under a fluorescence microscope and the number of (1) total, (2) active-caspase-3-positive and, (3) flat and active-caspase-3-positive cells was recorded. More than 300 cells were counted for each experimental condition.

Preparation of subcellular fractions

Following treatments, the cells were rinsed with cold PBS, scraped off and collected by centrifugation at 100 ***g*** (Beckman GS-6R, Beckman Canada, Mississauga, ON, Canada). Cells were resuspended and sonicated in PBS containing phosphatase and protease inhibitors {1 mM EDTA, 1 mM PMSF, 2 μg/ml leupeptin, 2 μg/ml aprotinin, 4 mM Na_3VO_4, 80 mM NaF, 20 mM $Na_4P_2O_7$ and 10 μM bisperoxovanadium 1,10-phenanthroline [bpV(phen)]}. The total cell homogenate was centrifuged to remove the nuclei and cell debris. After centrifugation, the supernatant was incubated with 1% Triton X-100 (final concentration) in PBS that contained phosphatase and protease inhibitors for 30 minutes at room temperature, followed by a centrifugation at 15,000 ***g*** (Beckman microfuge E, Beckman Canada, Mississauga, ON, Canada). The pellet was considered the cytoskeleton-enriched fraction and the supernatant the non-cytoskeleton-enriched fraction. The cytoskeleton fractions were dissolved in RIPA buffer (150 mM NaCl, 1% NP-40, 0.5% DOC, 0.1% SDS, 50 mM Tris pH 8). The characterisation of subcellular fractions had been be done and described before (Zheng et al., 2005).

Electrophoresis and immunoblotting

Fifteen micrograms of sample proteins were loaded onto 8-12% polyacrylamide gels. After electrophoresis, the proteins were transferred onto nitrocellulose membranes. Membranes were quickly stained with Ponceau Red to ensure equal loading, rinsed and blocked in PBS containing 5% milk and 0.1% Tween for 1 hour at room temperature. Membranes were incubated with the first antibody in PBS with 5% milk and 0.1% Tween, followed by incubation with the corresponding secondary antibody coupled to HRP. The antigen-antibody reactions were revealed by chemiluminescence. Bands on the films were scanned and the intensity of the bands was quantified by using the Scion Image Program (Scion Corporation, MD).

Co-immunoprecipitation studies

Co-immunoprecipitation studies were performed essentially as described before (Meilleur et al., 2007). Briefly, following treatments, cells were washed with cold PBS, scraped and collected by centrifugation at 100 ***g*** (Beckman GS-6R). Cells were incubated with lysis buffer [150 mM NaCl, 20 mM Tris-HCl pH 7.4, 1% NP-40, 100 μM PMSF, 5 mg/ml leupeptin, 5 μg/ml aprotinin, 10 μM bpV(pfen)] for 1 hour at 4°C. The cell lysate was centrifuged for 15 minutes at 15,000 ***g***, and 1 ml of supernatant was incubated with 100 μl of proteinA-Sepharose bead slurry (50%) at 4°C for 10 minutes on a rocker to pre-clear the cell lysate. ProteinA-Sepharose beads were removed by centrifugation at 15,000 ***g*** at 4°C for 10 minutes. Protein concentration in the pre-cleared lysates was determined by the method of Bradford. Pre-cleared supernatants (1 mg protein) were incubated with 100 μl of proteinA-Sepharose beads pre-incubated with either goat or rabbit anti-PKCζ antibody or anti-MHCIIB at 4°C overnight on a rocker. Beads were rinsed several times in lysis buffer, and were finally resuspended in 60 μl electrophoresis sample buffer (2×) and boiled for 5 minutes. After centrifugation at 15,000 ***g*** at 4°C, the supernatant was subjected to SDS-PAGE. After electrophoresis and transfer, the membrane was incubated with anti-MHCIIB or anti- PKCζ antibodies. Controls for the immunoprecipitation studies included incubation of the protein lysate with ProteinA-Sepharose4B beads not pre-incubated with the PKCζ or MHCIIB antibodies, the use of two different PKCζ antibodies to co-immunoprecipitate MHCIIB and the use of an antibody that did not pull down PKCζ or MHCIIB, such as anti-vimentin.

We thankfully acknowledge the generous gift of the TtT/GF cell line from U. Renner (Max-Plank Institute of Psychiatry, Munich, Germany) and of the MHCIIB$^{-/-}$ and control mouse embryonic fibroblasts from R. S. Adelstein (Laboratory of Molecular Cardiology, National Heart, Lung and Blood Institute, NIH, Bethesada, MD). We are grateful to the Developmental Studies Hybridoma Bank from the University of Iowa, Department of Biological Sciences for providing us with the antibody CMII 23 against MHCIIB. We express our sincere gratitude to R.-Marc Pelletier for his editorial assistance and helpful comments. The technical assistance of C. Charbonneau for the microscopy studies is very much appreciated. This work was funded by the Natural Sciences and Engineering Research Council of Canada to M.L.V., who is supported by a scholarship from Fonds de la recherche en santé du Québec.

References

Allaerts, W. and Vankelecom, H. (2005). History and perspectives of pituitary folliculostellate cell research. *Eur. J. Endocrinol.* **153**, 1-12.

Amano, M., Ito, M., Kimura, K., Fukata, Y., Chihara, K., Nakano, T., Matsuura, Y. and Kaibuchi, K. (1996). Phosphorylation and activation of myosin by rho-association of myosin by rho-associated kinase (Rho-kinase). *J. Biol. Chem.* **271**, 20246-20249.

Bao, J., Jana, S. S. and Adelstein, R. S. (2005). Vertebrate nonmuscle myosin II isoforms rescue small interfereing RNA-induced defects in COS-7 cell cytokinesis. *J. Biol. Chem.* **280**, 19594-19599.

Baud, V. and Karin, M. (2001). Signal transduction by tumor necrosis factor and its relatives. *Trends Cell Biol.* **11**, 372-377.

Boivin, P., Galand, C. and Dhermy, D. (1990). *In vitro* digestion of spectrin, protein 4.1 and ankyrin by erythrocyte calcium dependent neutral protease (Calpain l). *Int. J. Biochem.* **22**, 1479-1489.

Brancolini, C., Lazarevic, D., Rodriguez, J. and Schneider, C. (1997). Dismantling cell-cell contacts during apoptosis is coupled to a caspase-dependent proteolytic cleavage of βcatenin. *J. Cell Biol.* **139**, 759-771.

Bresnick, A. R. (1999). Molecular mechanisms of nonmuscle myosin-II regulation. *Curr. Opin. Cell Biol.* **11**, 26-33.

Chen, Y.-R., Kori, R., John, B. and Tan, T.-H. (2001). Caspase-mediated cleavage of actin- binding and SH3-domain-containing proteins, cortactin, HS1, and HIP-55 during apoptosis. *Biochem. Biophys. Res. Commun.* **288**, 981-989.

Coleman, M. L. and Olson, M. F. (2002). Rho GTPase signalling pathways in the morphological changes associated with apoptosis. *Cell Death Differ.* **9**, 493-504.

Coleman, M. L., Sahai, E. A., Yeo, M., Bosch, M., Dewart, A. and Olson, M. F. (2001). Membrane blebbing during apoptosis results from caspase-mediated activation of ROCK I. *Nat. Cell Biol.* **3**, 339-345.

Croft, D. R., Coleman, M. L., Li, S., Robertson, D., Sullivan, T., Steward, C. L. and Olson, M. F. (2005). Actin-myosin-based contraction is responsible for apoptotic nuclear disintegration. *J. Cell Biol.* **168**, 245-255.

Dulyaninova, N. G., House, R. P., Betapudi, V. and Bresnick, A. R. (2007). Myosin-IIA heavy-chain phosphorylation regulates the motility of MDA-MB-231 carcinoma cells. *Mol. Biol. Cell* **18**, 3144-3155.

Earnshaw, W. C. (1995). Nuclear changes in apoptosis. *Curr. Opin. Cell Biol.* **5**, 337-343.

Even-Faitelson, L. and Ravid, S. (2006). PAK1 and aPKCζ regulate myosin II-B phosphorylation: a novel signaling pathway regulating filament assembly. *Mol. Biol. Cell* **17**, 2869-2881.

Fortin, M.-E., Pelletier, R.-M., Meilleur, M.-A. and Vitale, M. L. (2006). Modulation of GJA1 turnover and intercellular communication by pro-inflammatory cytokines in the anterior pituitary folliculo-stellate cell line TtT/GF. *Biol. Reprod.* **74**, 2-12.

Gallagher, P. J., Herring, B. P. and Stull, J. T. (1997). Myosin light chain kinases. *J. Muscle Res. Cell Motil.* **18**, 1-16.

Gerner, C., Fröhwein, U., Gotzmann, J., Bayer, E., Gelbmann, D., Bursch, W. and Schulte-Hermann, R. (2000). The Fas-induced apoptosis analyzed by high throughput proteome analysis. *J. Biol. Chem.* **275**, 39018-39026.

Golomb, E., Ma, X., Jana, S. S., Preston, Y. A., Kawamoto, S., Shoham, N. G., Goldin, E., Conti, M. A., Sellers, J. R. and Adelstein, R. S. (2004). Identification and characterization of nonmuscle myosin II-C, a new member of the myosin II family. *J. Biol. Chem.* **279**, 2800-2808.

Inoue, K., Matsumoto, H., Koyama, C. and Shibata, K. (1992). Establishment of a folliculo-stellate like cell line from a murine thyrotropic pituitary tumor. *Endocrinology* **131**, 3110-3116.

Jänicke, R. U., Ng, P., Sprengart, M. L. and Porter, A. G. (1998). Caspase-3 required for α-fodrin cleavage but dispensable for cleavage of other death susbtrates in apoptosis. *J. Biol. Chem.* **273**, 15540-15545.

Kato, M., Fukuda, H., Nonaka, T. and Imajob-Ohmi, S. (2005). Cleavage of nonmuscle myosin heavy chain-A during apoptosis in human Jurkat T cells. *J. Biochem.* **137**, 157-166.

Kawamoto, S. and Adelstein, R. S. (1991). Chicken nonmuscle myosin heavy chains: differential expression of two mRNA and evidence for two different polypeptides. *J. Cell Biol.* **112**, 915-924.

Kelley, C. W., Sellers, J. R., Gard, D. L., Bui, D., Adelstein, R. S. and Baines, I. C. (1996). Xenopus nonmuscle myosin heavy chain isoforms have different subcellular localizations and enzymatic activities. *J. Cell Biol.* **134**, 675-687.

Kimura, K., Ito, M., Amano, M., Chihara, K., Fukata, Y., Nakafuku, M., Yamamori, B., Feng, J., Nakano, T., Okawa, K. et al. (1996). Regulation of myosin phosphatase by rho and rho-associated kinase (Rho-kinase). *Science* **273**, 245-248.

Kobayashi, H., Fukata, J., Murakami, N., Usui, T., Ebisui, O., Muro, S., Hanaoka, K., Imura, H. and Nakao, K. (1997). Tumor necrosis factor receptors in the pituitary cells. *Brain Res.* **758**, 45-50.

Kolega, J. (1999). Turnover rates at regulatory phosphorylation sites on myosin II in endothelial cells. *J. Cell. Biochem.* **75**, 629-639.

Kolega, J. (2003). Asymmetric distribution of myosin IIB in migrating endothelial cells is regulated by a rho-dependent kinase and contributes to tail retraction. *Mol. Biol. Cell* **14**, 4745-4757.

Kolega, J. (2006). The role of myosin II motor activity in distributing myosin asymmetrically and coupling protrusive activity to cell translocation. *Mol. Biol. Cell* **17**, 4435-4445.

Kook, S., Kim, D. H., Shim, S. R., Kim, W., Chun, J.-S. and Song, W. K. (2003). Caspase-dependent cleavage of tensin induces disruption of actin cytoskeleton during apoptosis. *Biochem. Biophys. Res. Commun.* **303**, 37-45.

Korn, E. D. (2000). Co-evolution of head, neck and tail domains of myosin heavy chains. *Proc. Natl. Acad. Sci. USA* **97**, 12559-12564.

Lane, J. D., Allan, V. J. and Woodman, P. G. (2005). Active relocation of chromatin and endoplasmic reticulum into blebs in late apoptotic cells. *J. Cell Sci.* **118**, 4059-4071.

Leong, K. G. and Kaplan, A. (2000). Signaling pathways mediated by tumor necrosis factor alpha. *Histol. Histopathol.* **15**, 1303-1325.
Lo, C.-M., Buxton, D. B., Chua, G. C. H., Dembo, M., Adelstein, R. S. and Wang, Y. L. (2004). Nonmuscle myosin IIB is involved in the guidance of fibroblast migration. *Mol. Biol. Cell* **15**, 982-989.
Maekawa, M., Ishizaki, T., Boku, S., Watanabe, N., Fujita, A., Iwamatsu, A., Obinata, T., Ohashi, K., Mizuno, K. and Narumiya, S. (1999). Signaling from Rho to the actin cytoskeleton through protein kinases ROCK and LIM-kinase. *Science* **285**, 895-898.
Meilleur, M.-A., Akpovi, C. D., Pelletier, R.-M. and Vitale, M. L. (2007). TNF-α–induced anterior pituitary folliculostellate TtT/GF cell uncoupling is mediated by connexin 43 dephosphorylation. *Endocrinology* **148**, 5913-5924.
Mills, J. C., Stone, N. L., Erhardt, J. and Pittman, R. N. (1998). Apoptotic membrane blebbing is regulated by myosin light chain phosphorylation. *J. Cell Biol.* **140**, 627-636.
Mills, J. C., Stone, N. L. and Pittman, R. N. (1999). Extranuclear apoptosis: the role of the cytoplasm in the execution phase. *J. Cell Biol.* **146**, 703-707.
Murakami, N., Kotula, L. and Hwang, Y.-W. (2000). The distinct mechanisms for regulation of nonmuscle myosin assembly via the heavy chain: phosphorylation for MIIB and Mts binding for MIIA. *Biochemistry* **39**, 11441-11451.
Noda, M., Fukasawa-Yasuda, C., Moriishi, K., Kato, T., Okuda, T., Kurokawa, K. and Takuwa, Y. (1995). Involvement of rho in GTPγS-induced enhancement of phosphorylation of 20kDa myosin light chain in vascular smooth cells: inhibition of phosphatase activity. *FEBS Lett.* **367**, 246-250.
Orlando, K. A., Stone, N. L. and Pittman, R. N. (2006). Rho kinase regulates fragmentation and phagocytosis of apoptotic cells. *Exp. Cell Res.* **312**, 5-15.
Redowicz, M. J. (2001). Regulation of nonmusle myosins by heavy chain phosphorylation. *J. Muscle Res. Cell Motil.* **22**, 163-173.
Sellers, J. R. and Goodson, H. V. (1995). Motor proteins 2, myosin. *Protein Profile* **2**, 1323-1423.
Smith, L., Chen, L., Reylands, M. E., DeVries, T. A., Talanian, R. V., Omura, S. and Smith, J. B. (2000). Activation of atypical protein kinase C ζ by caspase processing and degradation by the ubiquitin-proteasome system. *J. Biol. Chem.* **275**, 40620-40627.
Smith, L., Wang, Z. and Smith, J. B. (2003). Caspase processing activates atypical protein kinase C zeta by relieving autoinhibition and destabilizes the protein. *Biochem. J.* **375**, 663-671.
Song, Y., Hoang, B. Q. and Chang, D. D. (2002). Rock-II-induced membrane blebbing and chromatin condensation require actin cytoskeleton. *Exp. Cell Res.* **278**, 45-52.
Straussman, R., Even, L. and Ravid, S. (2001). Myosin II heavy chain isoforms are phosphorylated in an EGF-dependent manner: involvement of protein kinase C. *J. Cell Sci.* **114**, 3047-3057.
Suarez-Huerta, N., Lecocq, R., Mosselmans, R., Galand, P., Dumont, J. E. and Robaye, B. (2000a). Myosin heavy chain degradation during apoptosis in endothelial cells. *Cell Prolif.* **33**, 101-114.
Suarez-Huerta, N., Mosselmans, R., Dumont, J. E. and Robaye, B. (2000b). Actin depolymerization and polymerization are required during apoptosis in endothelial cells. *J. Cell. Physiol.* **184**, 239-245.
Swailes, N. T., Colegrave, M., Knight, P. and Peckham, M. (2006). Non-muscle myosins 2A and 2B drive changes in cell morphology that occur as myoblasts align and fuse. *J. Cell Sci.* **119**, 3570.
Takahashi, M., Kawamoto, S. and Adelstein, R. S. (1992). Evidence for inserted sequences in the head region of nonmuscle myosin specific to the nervous system. Clonning of the cDNA encodeng the myosin heavy chain-B isoform of vertebrate nonmuscle myosin. *J. Biol. Chem.* **267**, 17864-17871.
Togo, T. and Steinhardt, R. A. (2004). Nonmuscle myosin IIA and IIB have distinct functions in the exocytosis-depedent process of cell membrane repair. *Mol. Biol. Cell* **15**, 688-695.
Tullio, A. N., Accili, D., Ferran, V. J., Yu, Z.-X., Takeda, K., Grinberg, A., Westphal, H., Preston, Y. A. and Adelstein, R. S. (1997). Nonmuscle myosin II-B is required for normal development of the heart. *Proc. Natl. Acad. Sci. USA* **94**, 12407-12412.
Vicente-Manzanares, M., Zareno, J., Whitmore, L., Choi, C. K. and Horwitz, A. F. (2007). Regulation of protrusion, adhesion dynamics, and polarity by myosins IIA and IIB in migrating cells. *J. Cell Biol.* **176**, 573-580.
Vitale, M. L. and Carbajal, M. E. (2004). Involvement of myosin II in dopamine-induced reorganization of the lactotroph cell's actin cytoskeleton. *J. Histochem. Cytochem.* **52**, 517-527.
Wei, Q. and Adelstein, R. S. (2000). Conditional expression of a truncated fragment of nonmuscle myosin II-A alters cell shape but not cytokinesis in HeLa cells. *Mol. Biol. Cell* **11**, 3617-3627.
Wilson, J. R., Ludowyke, R. I. and Biden, T. J. (2001). A redistribution of actin and myosin IIA accompanies Ca-dependent insulin secretion. *FEBS Lett.* **492**, 101-106.
Wylie, S. R. and Chantler, P. D. (2001). Separate but linked functions of conventional myosins modulate adhesion and neurite outgrowth. *Nat. Cell Biol.* **3**, 88-92.
Wylie, S. R. and Chantler, P. D. (2003). Myosin II A drives neurite retraction. *Mol. Biol. Cell* **14**, 4654-4666.
Zheng, G. F., Solinet, S., Pelletier, R.-M. and Vitale, M. L. (2005). Actin cytoskeleton remodelling in the anterior pituitary folliculo-stellate cell line TtT/GF: implication of the actin-binding protein cortactin. *J. Mol. Histol.* **36**, 461-474.